Effect of gold nanoparticles on structure and dynamics of binary Lennard-Jones liquid: Direct space analysis

L. Separdar and S. Davatolhagh*
Department of Physics, College of Sciences, Shiraz University, Shiraz 71454, Iran
(Received 23 September 2012; published 19 February 2013)

We investigate the static structure and diffusive dynamics of binary Lennard-Jones mixture upon supercooling in the presence of gold nanoparticle within the framework of the mode-coupling theory of the dynamic glass transition in the direct space by means of constant-*NVT* molecular dynamics simulations. It is found that the presence of gold nanoparticle causes the energy per particle and the pressure of this system to decrease with respect to the bulk binary Lennard-Jones mixture. Furthermore, the presence of nanoparticle has a direct effect on the liquid structure and causes the peaks of the radial distribution functions to become shorter with respect to the bulk binary Lennard-Jones liquid. The dynamics of the liquid at a given density is found to be consistent with the mode-coupling theory (MCT) predictions in a certain range at low temperatures. In accordance with the idealized MCT, the diffusion constants $D(T)$ show a power-law behavior at low temperatures for both types of binary Lennard-Jones (BLJ) particles as well as the gold atoms comprising the nanoparticle. The mode-coupling crossover temperature T_c is the same for all particle types; however, $T_c = 0.4$ is reduced with respect to that of the bulk BLJ liquid, and the γ exponent is found to depend on the particle type. The existence of the nanoparticle causes the short-time β-relaxation regime to shorten and the range of validity of the MCT shrinks with respect to the bulk BLJ. It is also found that at intermediate and low temperatures the curves of the mean-squared displacements (MSDs) versus $tD(T)$ fall onto a master curve. The MSDs follow the master curve in an identical time range with the long-time α-relaxation regime of the mode-coupling theory. By obtaining the viscosity, it is observed that the Stokes-Einstein relation remains valid at high and intermediate temperatures but breaks down as the temperatures approach T_c as a result of the cooperative motion or activated processes.

DOI: 10.1103/PhysRevE.87.022305 PACS number(s): 64.70.pm, 52.35.Mw, 31.15.xv

I. INTRODUCTION

The problem of the viscous liquids and glass transition is a classic one in the condensed matter physics. Systems on approaching the glass transition, exhibit common features that seem to hold for liquids with different kinds of chemical bonding. Inorganic and organic compounds can form glasses, as can polymeric and metallic systems. The universal features relate to the temperature dependence of the viscosity and to the time dependence of the relaxation functions. It is, therefore, useful to have a standard model system as a reference. For many years, the Kob-Andersen 80-20 Binary Lennard-Jones (BLJ) mixture has served this purpose [1]. This model has not been found to crystallize for temperatures above $T = 0.45$ (BLJ units), although more recently it has been shown that in long enough simulations in the temperature interval (0.39,0.45) the system phase separates and A particles crystallize [2]. A convenient framework for interpreting the behavior of lightly supercooled liquids close to their melting point, is provided by the mode-coupling theory (MCT). The MCT first proposed by Bengtzelius, Götze and Sjölander [3], interprets the kinetic slow down as an artifact of an avoided dynamic transition. This theory predicts the dynamics of the liquid from its structure, and it has found support in both laboratory liquids (see Ref. [4], and the references therein) as well as numerical simulations of model systems [5]. However, this theory has some failures, the most notable of which is the inability to explain the observed behavior of deeply supercooled liquids close to their laboratory glass transition temperature T_g [6]: the MCT is, therefore, a theory of lightly supercooled liquids. Also MCT fails to explain the collective relaxation and the breakdown of the Stokes-Einstein relation [7]. Nevertheless, MCT is also formally born out of the mean-field p-spin glass models [8], which exhibit a thermodynamic random first order transition at a temperature T_K less than T_c and provide for an alternative viewpoint on structural glasses [9], in particular, the problem of deep supercooling.

Kob and Andersen have discussed in detail the unusual features of BLJ upon supercooling [5] within the framework of the MCT both in the direct and the reciprocal space. More recently, Gallo *et al*. investigated the MCT predictions for the (confined) BLJ molecules, embedded in an off-lattice matrix of fixed nanoscale soft spheres both in the direct- and the Q-space [10]. Now the question we ask is how accurate are the predictions of MCT for the BLJ fluid in the presence of a nanoparticle such as gold that is free to move through the liquid. In this work we attempt to answer this question. The motivation comes from the increasing utility of nanoparticles in glassy materials and the need for understanding the physics of such systems at the molecular level. In fact, as the filler size enters the nanoscale, the increasing interface area of the liquid and the nanofillers becomes the basis for tremendous changes in the liquid properties. For example, in Ref. [11] the presence of gold nanoparticle in polymer polyoctylthiophene alters the morphological and spectral features of the polymer. Furthermore, the effect of nanoparticle on dynamics and structure of supercooled liquids is studied via simulation [12], and x-ray photon correlation spectroscopy [13]. In Refs. [14,15], the silicate nanoparticle is found to significantly

*davatolhagh@susc.ac.ir

affect the diffusion of the polymer, and the high surface of the silica raises the effective glass transition temperature of the polymer matrix, while in numerical simulations it is found that the effective glass transition temperature can be either raised or reduced by tuning the interaction between the nanoparticle and the polymer [12].

In this work, we investigate by means of molecular dynamics simulations the effect of gold nanoparticle on structure and dynamics of the most studied model of glass forming liquids, i.e., the binary Lennard-Jones fluid, within the framework of the mode-coupling theory in the direct space. The MCT predictions have been tested for the bulk phase of the BLJ in detail [5]. We present the results of constant-*NVT* molecular dynamics simulations in the direct space to find the range of validity of the MCT in the presence of gold nanoparticle and to compare results with the bulk BLJ. The rest of this paper is organized as follows. In Sec. II the main predictions of the mode-coupling theory relevant to our work are briefly reviewed. In Sec. III, we introduce the model system and describe the simulation methodology. In Sec. IV, the simulation results for the static and the dynamic properties of the system are presented and compared with those of the bulk BLJ. The paper is concluded with a discussion and summary in Sec. V.

II. MODE-COUPLING THEORY

We briefly review some predictions of the mode-coupling theory that are relevant for the interpretation of the results presented in this paper. Extensive reviews can be found, e.g., in Refs. [16,17]. The idealized MCT provides an equation of motion for the time correlation functions, which uses static correlations and interaction potentials as the input. The MCT works under the hypothesis that the knowledge of the pair correlation function $g(r)$ of the fluid (or its Fourier transform, the static structure factor), is sufficient to predict the dynamical evolution of time-correlation functions. In this theory, a dynamic feedback mechanism caused by nonlinear coupling of the slow modes, self-consistently produces very slow dynamics. As a result of this feedback mechanism a dynamic transition of the liquid to a nonergodic state is predicted. This apparent dynamic transition from ergodic to nonergodic state occurs at a critical temperature T_c below the melting temperature. In real systems, however, the dynamical arrest is averted by the cooperative motion or the activated hopping mechanism that is not included in the ideal form of the MCT. In a temperature range above T_c, where the activated processes can be neglected, and below an onset temperature T_{on}, where the slow dynamics regime sets in [18], the MCT fares quite well to describe a host of experimental and numerical results. One of the main predictions of MCT within this regime is that the translational diffusion has a power-law dependence on temperature:

$$D \sim (T - T_c)^{\gamma}. \tag{1}$$

In its ideal version, the MCT also predicts that the curves of dynamic properties such as correlation functions versus logarithmic response time for different temperatures can be superimposed by shifts of curves parallel to the logarithmic reduced time, i.e., $t/\tau(T)$ axis, where $\tau(T)$ is the associated relaxation time at temperature T. This law is valid only for the long-time α-relaxation regime that characterizes the structural relaxation; the short-time β-relaxation or the cage-rattling regime, does not scale in the same manner. This specific long-time α-relaxation scaling law is also called the time-temperature superposition principle:

$$\phi(t,T) = F[t/\tau(T)], \tag{2}$$

where $F[t/\tau(T)]$ is a master curve that the correlation functions $\phi(t)$ for different temperatures fall onto. These predictions are valid only when hopping processes can be neglected [7,19,20].

III. SYSTEM DESCRIPTION AND SIMULATION METHODOLOGY

The system considered in this work, abbreviated by BLJ + Gold, consists of a binary mixture of classical particles composed of 800 particles of type A and 200 particles of type B with masses $m_A = m_B = 1$ in the presence of a gold nanoparticle composed of 13 gold atoms (called C particles) with a total mass $64\,m_A$. All particles are placed inside a cubic box with an edge length $L = 9.486\,\sigma_A$, in constant volume. Periodic boundary conditions were applied. The basic pair interaction is that of the Lennard-Jones potential

$$V(r) = 4\epsilon_{\mu\nu}[(\sigma_{\mu\nu}/r)^{12} - (\sigma_{\mu\nu}/r)^{6}], \tag{3}$$

where indices μ and ν run on the particle types A, B, and C. The values of the parameters for A and B particles are those of the Kob-Andersen mixture, which are similar to the parameters proposed by Weber and Stillinger to describe amorphous $Ni_{80}P_{20}$ [21], and the corresponding values for gold nanoparticle are those referenced in Ref. [22]. The parameters of interactions between the BLJ particles and the C particles are obtained from the Lorentz-Berthelot combination rules

$$\sigma_{\mu\nu} = (\sigma_\mu + \sigma_\nu)/2 \tag{4}$$

and

$$\epsilon_{\mu\nu} = \sqrt{\epsilon_\mu \epsilon_\nu}. \tag{5}$$

The potential parameters for different pair interactions are listed in Table I.

The potentials are truncated and shifted at a distance of $2.5\,\sigma_A$. In the following, all the results will be given in the usual BLJ (reduced) units such that length is measured in units of σ_A, energy in units of ϵ_A, and time in units of $\sqrt{m\sigma_A^2/48\epsilon_A}$. The temperature has ϵ_A/k_B as its unit, where k_B is the Boltzmann constant.

TABLE I. The mutual interaction parameters between A, B, and C particles in BLJ units.

Atom pair	σ	ε
A-A	1	1
B-B	0.88	0.5
C-C	0.77	22.18
A-B	0.80	1.5
A-C	0.885	4.814
B-C	0.825	3.33

We performed equilibrium molecular dynamics (MD) simulations in the canonical ensemble using the Nosé-Hoover thermostat within the framework of RUMD and Gromacs molecular dynamics simulation softwares [23]. The gold nanoparticle was first generated by a process of simulated annealing in which starting from a high-T configuration, the temperature of the 13 gold atoms was gradually reduced until the low-T equilibrium configuration was obtained. The resulting nanoparticle was then inserted into the BLJ fluid. The shape of the gold nanoparticle so obtained is identical with that reported in Ref. [24] for 13 gold atoms. The system was simulated in a temperature range $0.4 \leqslant T \leqslant 4$ with the number density of the BLJ particles (A and B particles without the gold nanoparticle) held at a constant value $1.2/\sigma_A^3$, which is the same as the density reported in Ref. [5] for the bulk BLJ. The integration time step used is 0.002 BLJ units. The simulations were started at the highest temperature, $T = 4$, where the relaxation time is short. Then the temperature of the system was reduced stepwise by coupling it to a Nosé-Hoover thermostat. For every temperature, the final equilibrium state of the system at the adjacent higher temperature was used as the initial configuration. In order to check whether the system is equilibrated, we plotted the thermodynamic functions such as the total energy, the potential energy, and the pressure as functions of time. If no drift was found, we concluded that the system is in equilibrium. The temperatures studied correspond to $T = 4$, 3, 2.5, 2, 1.5, 1, 0.8, 0.7, 0.6, 0.55, 0.5, 0.47, 0.45, 0.42, and 0.4. The results reported refer to the system of BLJ + Gold, unless otherwise stated.

IV. RESULTS

In this section the results of the simulations are presented. In the first part we report the static properties, and in the second part the time-dependent quantities are presented.

A. Static properties

Figure 1 shows the thermodynamics such as the internal energy per particle, the average potential energy per particle, and the pressure of the system as a function of the reciprocal temperature. From the smoothness of the curves, it is evident that there are no thermodynamic anomalies and the system is in equilibrium down to the lowest temperatures investigated. A similar trend was observed in the bulk BLJ [5]; however, the values of the total energy and the potential energy are reduced with respect to the bulk BLJ. At high temperatures, an average decrease of about $1.25\,\epsilon_A$ of the total energy and of the potential energy is found with respect to the bulk BLJ. This difference tends to reduce gradually to $1.14\epsilon_A$ upon cooling. This decrease in the values of the total energy and the potential energy with respect to the bulk BLJ is related to the presence of the gold nanoparticle that strongly attracts the BLJ particles, in particular, the majority A particles. The pressure is reduced by 2 reduced units at high temperatures and 0.98 at low temperatures, compared to the bulk BLJ.

The radial distribution functions of the AA, BB, AB, CA, CB, and CC pairs for the entire temperature range $0.4 \leqslant T \leqslant 4.0$ are shown in Fig. 2. In the figure, the curves for different temperatures are shifted vertically by $0.1n$ ($n = 1,2,3,\ldots$) for clarity, except for $g_{CC}(r)$, which is shifted by $5n$. As shown in Fig. 2(a), by decreasing the temperature, the first neighbor peak for the majority A particles becomes sharper and moves slightly to higher values of r and the second peak starts to split around $T \simeq 0.7$, which also corresponds to the onset of slow dynamics as described in Sec. IV B. Clearly, there is no indication of phase separation. This phenomenon would in fact result in a substantial decrease of the area under the first peak of $g_{AB}(r)$. The occurrence of a split second-neighbor peak indicates that the system is in the supercooled liquid phase, and the local packing increases with decreasing temperature such that an extended local order begins to develop in the system. In this regard, there is no significant difference between our system of BLJ + Gold and bulk BLJ apart from the fact that on lowering the temperature the height of the first-neighbor peak decreases in comparison with the bulk. The inset of Fig. 2(a) shows this decrease in the height of the first peak in $g_{AA}(r)$ at $T = 0.45$ (dashed line) with respect to the bulk BLJ (solid line). Although this reduction is small, we found it to become more pronounced by increasing the nanoparticle size. This effect that is also found in $g_{AB}(r)$ and $g_{BB}(r)$ may be attributed to the gold nanoparticle that tends to attract the BLJ particles A and B toward itself, and the effect becoming more discernible with lowering temperature.

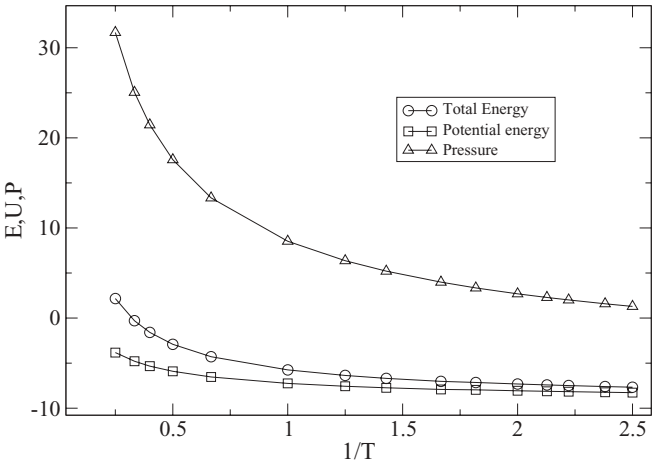

FIG. 1. Thermodynamics of binary Lennard-Jones in the presence of gold nanoparticle. The internal energy per particle, E, the average potential energy per particle, U, and the pressure, P, are plotted as a function of the inverse temperature. There is no sign of a thermodynamic anomaly or phase transition.

In Fig. 2(b), $g_{BB}(r)$ shows the behavior of the pairs of minority B particles and their local packing structure, which is quite different from that of a simple one-component liquid. On lowering the temperature, this first peak shrinks and becomes a small shoulder, while the first peak of $g_{AB}(r)$ increases. This behavior relates to the fact that attraction between A and B particles is more than that among the B particles. Despite this behavior, the second peak of $g_{BB}(r)$ becomes much larger and splits at temperatures around the onset $T \simeq 0.7$. A comparison of our system with the bulk BLJ reveals that in the case of $g_{BB}(r)$ the height of the second peak in the presence of the gold nanoparticle is lower than that in the bulk BLJ. Functions $g_{CA}(r)$ and $g_{CB}(r)$ represent the correlation between the majority A and the minority B

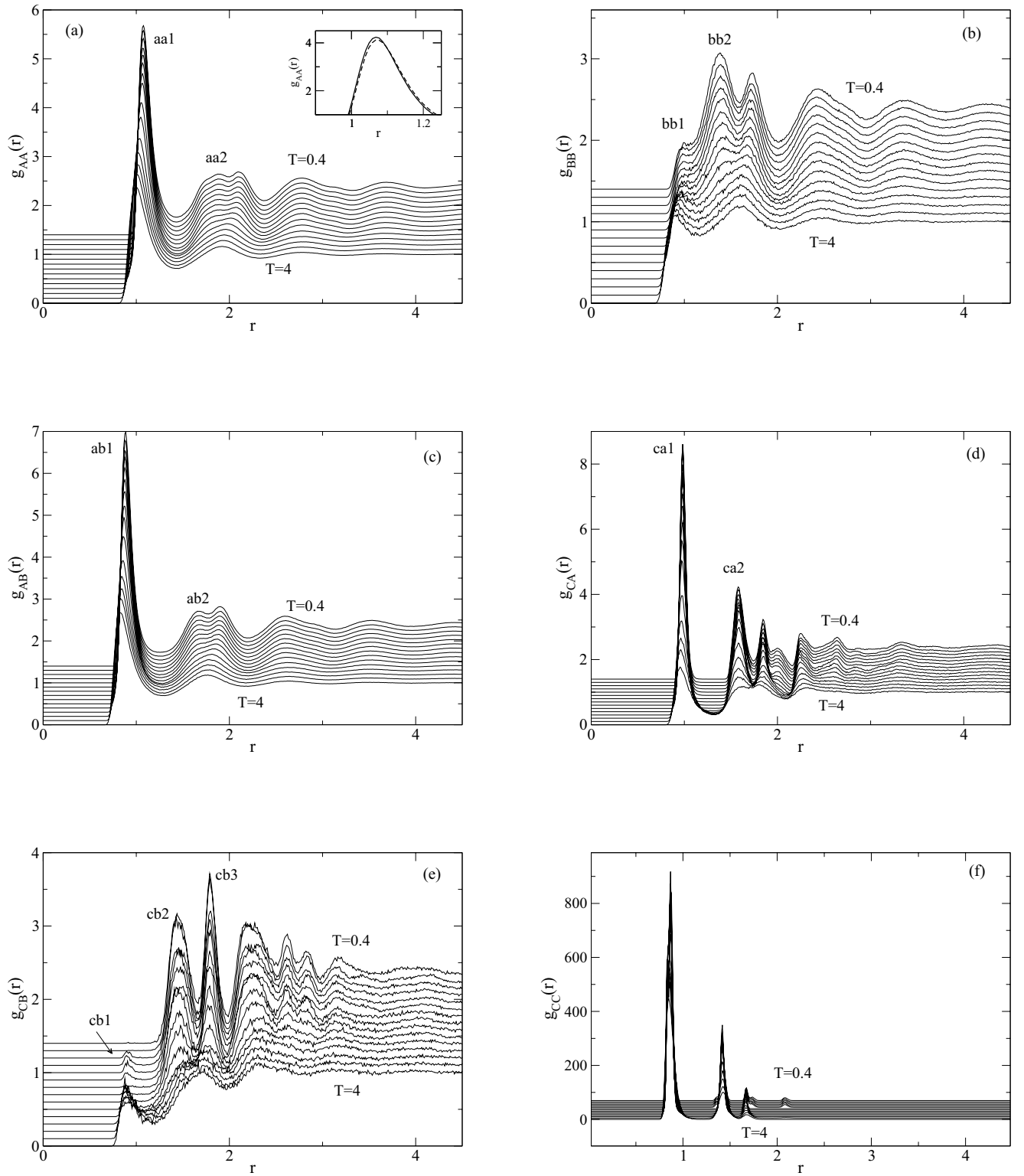

FIG. 2. The radial distribution functions for AA, BB, AB, CA, and CB pairs at different temperatures: (f) represents the structure of 13 gold atoms, which form the nanoparticle. For clarity, the individual curves have been shifted vertically by $0.1n$ ($n = 1,2,\ldots$) except for $g_{CC}(r)$, which is shifted vertically by $5n$. The inset of $g_{AA}(r)$ compares the height of the first peak in our system of the BLJ + Gold (dashed line) with that in the bulk BLJ (solid line).

particles with the gold nanoparticle, respectively. The behavior of $g_{CA}(r)$ shows that on decreasing the temperature, the A particles tend to be adsorbed on the nanoparticle surface. The A particles create a solid-like layer around the gold nanoparticle. A similar behavior has been reported in Refs. [25–27]. We note the gradual disappearance of the first peak of the $g_{CB}(r)$

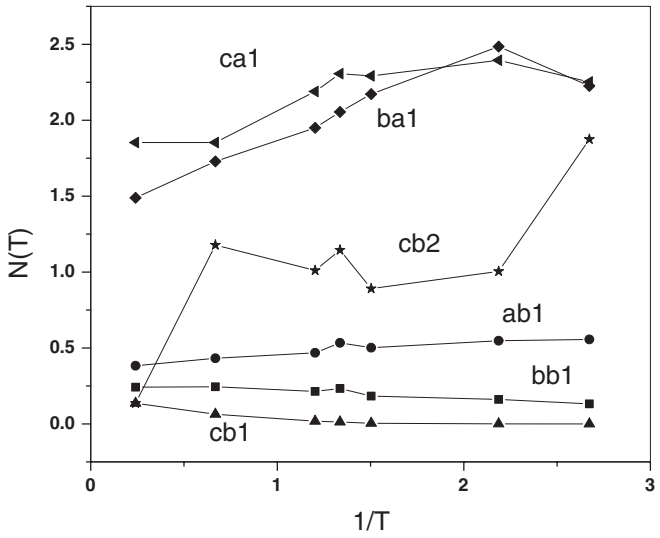

FIG. 3. The coordination numbers obtained from the peaks of the radial distribution functions as a function of inverse temperature.

for temperatures $T \lesssim 0.7$, which is accompanied by the enhancement of the first peak of $g_{\mathrm{CA}}(r)$. The structure of the mixture is such that the CA and CB peaks alternate in space. Figure 2(f) demonstrates the radial distribution of gold nanoparticle comprising 13 gold atoms. By decreasing the temperature, the $g_{\mathrm{CC}}(r)$ peaks become sharper, indicating more order in the local structure of the 13 gold atoms that form a nearly rigid ensemble. However, a fourth diminished peak also appears that is due to the perturbations caused by the A particles that create a layer around the nanoparticle, thus disturbing its shape. We calculated the cumulative number that is the average number of particles within each coordination shell

$$N_{\mu\nu}(r_1,r_2) = 4\pi\rho x_\nu \int_{r_1}^{r_2} r^2 g_{\mu\nu}(r)dr, \qquad (6)$$

where ρ is the number density, x_ν is the relative fraction of the particles of type ν, and $g_{\mu\nu}(r)$ is the radial distribution function of the pair in question. This quantity as a function of temperature can help to quantify the above observations for the radial distribution functions, as it demonstrates the changes in various coordination numbers with lowering temperature. Figure 3 shows this quantity evaluated for certain peaks. The figure shows the number of B particles around the nanoparticle in the first shell (cb1). This number lowers upon decreasing the temperature in favor of an increase in the second shell (cb2), while the number of A particles in the first shell (ca1) also increases. This alternating arrangement of A and B particles around the gold nanoparticle relates to the fact that the attraction between A and C particles characterized by ϵ_{CA} is more than that between B and C particles or ϵ_{CB}. In turn, the A particles adsorbed on the gold nanoparticle tend to attract the B particles more strongly than the other A particles.

B. Dynamic quantities

Figure 4(a) shows the log-log plot of the mean-squared displacement (MSD) $\langle r^2(t)\rangle$ of A particles versus time for our system of BLJ + Gold. For short times, the MSDs are proportional to t^2. This regime corresponds to the ballistic motion. At the onset of the diffusive motion, the MSDs become proportional to t. At high temperatures the ballistic motion goes over immediately into a diffusive motion, but for temperatures below the onset of slow dynamics $T_{\mathrm{on}} \simeq 0.7$, the MSDs do not immediately switch to diffusive regime after the ballistic motion, and a plateau appears at intermediate times due to the cage effect of the neighboring coordination shells. This plateau indicates that the system is approaching a glass transition. We note that the dynamic crossover temperature $T_{\mathrm{on}} \simeq 0.7$, at which a plateau begins to appear, also corresponds to the temperature at which the second peaks in radial distribution functions begin to split, which is indicative of the extended local order that starts to develop in the liquid. From the height of the plateau, one can estimate the cage radius. The value obtained for both A and B particles is about $\langle r^2\rangle = 0.04$, corresponding to a root-mean-square distance of 0.2, which happens to be very similar to that found in the bulk BLJ. Within this distance, a tagged particle traps in a cage of its nearest neighbors. The time extension of this plateau enhances upon lowering the temperature. The inset of Fig. 4(a) demonstrates the MSDs at $T = 0.45$ for both our system of the BLJ + Gold (upper dashed curve) and the bulk BLJ (lower solid curve) for comparison. The β-relaxation regime corresponding to the plateau is shorter than that in the bulk BLJ. Figure 4(b) shows the MSDs for A and B particles for comparison. The larger A particles diffuse slower than the B particles, and this effect becomes more pronounced with lowering the temperature as the A particles tend to create a layer around the nanoparticle.

The diffusive motion of simple liquids in equilibrium is restored after leaving the plateau. A linear fit to this long-time regime gives the diffusion constant D according to the Einstein relation $\langle r^2(t)\rangle = 6Dt$. The results for the diffusion constants in the range of temperatures investigated are shown in Fig. 5 for A, B, and C particles. A and B particles behave in a similar way, but as the temperature is reduced, the ratio of the diffusion coefficients $D(\mathrm{B})/D(\mathrm{A})$ changes from 1.4 at $T = 4$ to 4.15 at $T = 0.4$. The diffusion of the 13 gold atoms (C particles) comprising the nearly rigid nanoparticle at high temperatures can be determined in the same way as the A and B particles (i.e., by a linear fit to the long-time regime of the corresponding MSD curve); however, on decreasing the temperature below the onset of slow dynamics $T_{\mathrm{on}} \simeq 0.7$, it gets harder for the gold nanoparticle to get rid of the neighboring A particles and to break out of its cage as a result of the high attractive potential and the low temperature. In this regime of temperatures, it is difficult to accurately calculate the diffusion of C particles from the slope of the corresponding MSD curves, and the data shown in Fig. 5 for C particles below $T_{\mathrm{on}} \simeq 0.7$ must be regarded as a rough estimate. Nevertheless, they are shown to give an overall picture of the diffusion of C particles. The main point being that the gold nanoparticle consistent with the MCT behaves in a similar manner as the A and B particles even at low temperatures. As pointed out in Sec. II, for temperatures approaching T_c, the MCT predicts that the diffusion constants must have a power-law dependence on temperature. From the temperature dependence of the diffusion coefficients, we can test this prediction of the MCT as given by Eq. (1). In Fig. 5, the fits to the MCT power law are also shown. Our best estimates of T_c are 0.40(1) for A particles, 0.40(2) for B particles, and

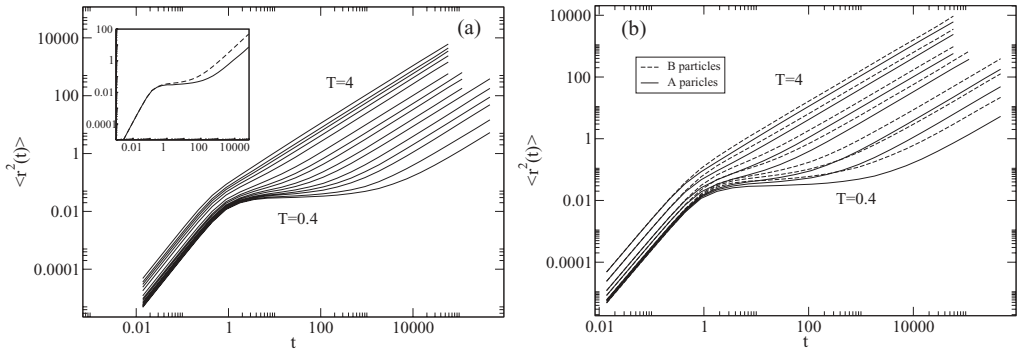

FIG. 4. (a) The logarithmic plot of the mean-squared displacement of A particles for the entire temperature range investigated. Inset shows a comparison of the MSDs for bulk BLJ (solid curve) and BLJ + Gold (dashed curve) at a temperature $T = 0.45$. (b) The MSDs of A and B particles are shown at temperatures $T = 4$, 2, 1, 0.7, 0.5, 0.45, and 0.4 for comparison. In the entire temperature range, the B particles diffuse faster than the A particles.

0.40(6) for C particles. This independence of the T_c from the particle type is in excellent agreement with the predictions of MCT. The exponent γ is found to be 1.94(11) for A particles, 1.57(10) for B particles, and 2.02(33) for C particles. The range of validity of the MCT in terms of the reduced distance from the apparent dynamic transition point $\epsilon = (T - T_c)/T_c$, is $0.05 < \epsilon < 0.75$, corresponding to the temperature range $0.42 < T < 0.7$ used for the straight line fits shown in Fig. 5. The range of validity of the MCT reported for bulk BLJ is much wider: $0.07 < \epsilon < 1.3$. The deviation from the power-law behavior for temperatures below the lower limit, $T = 0.42$, is accounted for by the developing cooperative motion or activated hopping that is not included in the ideal form of the MCT. To investigate the extent of this cooperative dynamical effect, in Fig. 6 the non-Gaussianity parameter is reported,

$$\alpha_2(t) = \frac{3\langle r^4(t)\rangle}{5\langle r^2(t)\rangle^2} - 1, \tag{7}$$

which is a measure of the deviation from the simple diffusive motion that is characterized by a Gaussian profile such that $\alpha_2(t) = 0$. The figure shows that on the timescale of our simulations, $t = 1.2 \times 10^5$ BLJ time units, the deviation from homogeneous diffusion is negligible, except for the lowest two temperatures investigated, $T = 0.4$ and 0.42. The apparent dynamic transition temperature for our system, $T_c = 0.4$, is lower than that of the bulk BLJ because of the presence of a gold nanoparticle that tends to adsorb the A and B particles, as a result of which in the proximity of the nanoparticle the local density increases and more space (free volume) will be available for the other BLJ particles that are further away from the gold nanoparticles, and so their mobility increases resulting in a reduced T_c. The inset of Fig. 5 shows the diffusion D of A and B particles as a function of temperature in Bulk

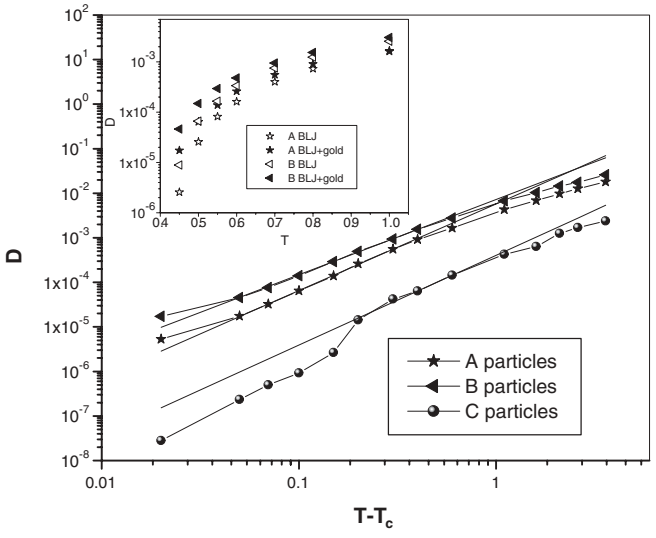

FIG. 5. The diffusion coefficients versus shifted temperature for A, B, and C particles comprising the gold nanoparticle. The straight lines correspond to the MCT fits of Eq. (1). The values of fit parameters are found to be $T_c = 0.4$ for all particle types, while the γ exponent is 1.94 for A particles, 1.57 for B particles, and 2.02 for C particles. The inset shows the diffusion of A and B particles in Bulk BLJ (empty symbols) and BLJ + Gold (solid symbols) for comparison, as a function of the temperature.

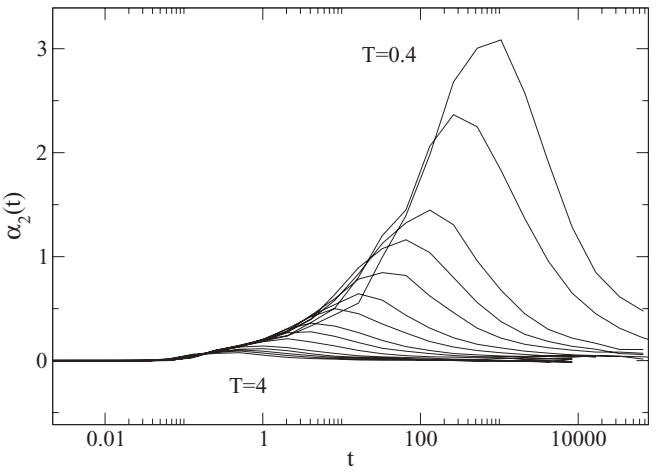

FIG. 6. The non-Gaussianity parameter $\alpha_2(t)$ that is a measure of the cooperative motion or dynamic heterogeneity. The small values found for $\alpha_2(t)$ on the time scale of our simulations, $t = 1.2 \times 10^5$ BLJ time units, is indicative of the fact that the dynamics of our system is mainly homogeneous, except for the lowest two temperatures, $T = 0.4$ and 0.42.

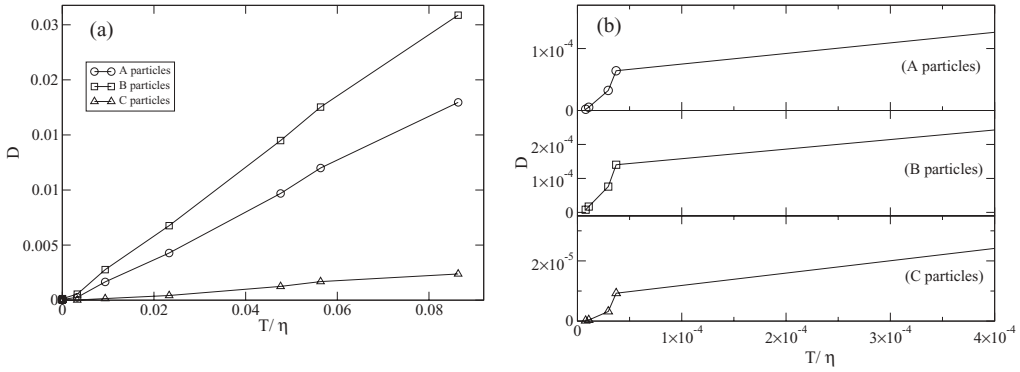

FIG. 7. (a) The diffusion D versus T/η for A, B, and C particles comprising the gold nanoparticle. The Stokes-Einstein relation is well obeyed at high and intermediate temperatures. (b) A blow up of the same function is shown at the lowest four temperatures, $T = 0.5$, 0.47, 0.42, and 0.4, for A, B, and C particles. Clearly, there is a deviation from straight line at the lowest temperatures, indicating a break down of the Stokes-Einstein relation on deep supercooling.

BLJ (empty symbols) and BLJ + Gold (solid symbols) for comparison. Clearly, the structural changes affected by the gold nanoparticle have enhanced the diffusion of A and B particles in comparison with bulk BLJ.

We computed the viscosity η as the integrated shear stress autocorrelation function within the framework of the Green-Kubo formalism:

$$\eta = \frac{V}{k_B T} \int_0^\infty \langle \sigma_{xy}(0)\sigma_{xy}(t)\rangle dt, \tag{8}$$

where σ_{xy} is the off-diagonal element of the stress tensor, and angular braces denote equilibrium ensemble average. One of the most important aspects of the phenomenology of supercooled liquids is the breakdown of the Stokes-Einstein relation. The Stokes-Einstein relation $D = k_B T/6\pi\eta R$ states that the slope of the curve of the self-diffusion constant D versus the temperature divided by the viscosity η is a constant. Figure 7(a) shows the diffusion versus T/η for A, B, and C particles. Figure 7(b) shows the same function zoomed in at the lowest four temperatures investigated, $T = 0.5$, 0.47, 0.42, and 0.4. Clearly, the Stokes-Einstein relation is well obeyed for temperatures $T > 0.42$, where the activated or cooperative processes are insignificant [28] on the timescale of our simulations as indicated by the non-Gaussianity parameter α_2 shown in Fig. 6. Instead, on further supercooling, and as the temperatures approach T_c, this relation breaks down as demonstrated in Fig. 7(b).

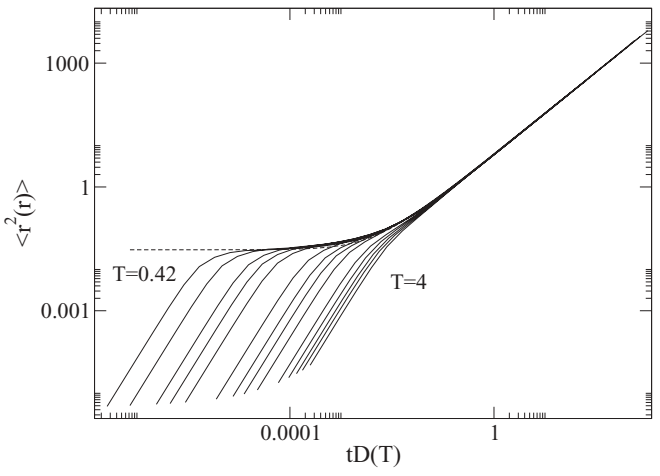

FIG. 8. The logarithmic plot of the mean-squared displacement versus $tD(T)$ for A particles. The curves to the right correspond to high temperatures, and those to the left relate to low temperatures. The dashed line is the best fit by Eq. (9).

In Fig. 8, we have plotted the MSDs of A particles as a function of $tD(T)$ for different temperatures. For times beyond the β-relaxation or the cage-rattling period, all curves fall onto a master curve. This region corresponds to the α-relaxation or the structural-relaxation regime. This master curve has to do with the time-temperature superposition principle of Eq. (2). Comparison between this plot and that of the bulk BLJ [5] indicates that A (as well as B) particles release from their cages in a shorter time interval than those in the bulk BLJ, which must be attributed to the changes in local structure affected by the gold nanoparticle, such that the increase in local density in proximity of the nanoparticle leaves more space for the diffusion of the particles further away from the nanoparticle. We use a three parameter fit function that was used previously by Kob and Andersen to fit a similar curve:

$$\langle r^2(t)\rangle = A\left[r_c^2 + (tD)^b\right] + tD. \tag{9}$$

In Eq. (9), r_c, A, and b are fitting parameters. The best value of b parameter is 0.919 for A particles and 0.909 for B particles. This fit is included in the plot of Fig. 8.

V. SUMMARY AND DISCUSSION

With the aid of canonical molecular dynamic simulations, changes of static and dynamic properties of Kob-Andersen binary Lennard-Jones liquid in the presence of a gold nanoparticle were explored. The direct space quantities have been analyzed upon supercooling for a test of the MCT behavior. The curves of the thermodynamic properties such as the total energy and pressure confirm that the liquid is in equilibrium for all temperatures investigated as no drift or sign of thermodynamic singularity was observed. However, the strong attractive potential of the gold nanoparticle causes the values of these quantities to decrease with respect to the bulk BLJ. The investigation of radial distribution functions of the AA, AB, and BB pairs led to similar conclusions as

in the bulk BLJ; however, $g_{CA}(r)$ and $g_{CB}(r)$ give evidence that the A particles create a layer around the nanoparticle, and the B particles avoid the surface of the gold nanoparticle as the temperature is reduced. This causes the B particles to move faster than A particles in the entire temperature range. Power-law fits to the diffusion coefficients extracted from the slope of the MSDs give an estimate of $T_c = 0.4$ for all A, B, and C particle types. The exponent γ is 1.94(11) for A particles, 1.57(10) for B particles, and 2.02(33) for C particles. The MCT predicts that the exponent γ is a universal exponent. However, these values of γ are consistent with those reported for the bulk BLJ: $\gamma = 2$ and 1.7 for A and B particles, respectively [5]. The MCT crossover temperature T_c, is reduced with respect to the bulk BLJ. The T_c depression is related to the enhanced mobility of A and B particles in the presence of gold nanoparticle, which adsorbs the BLJ particles, thus increasing the local density while leaving more free volume for other A and B particles further away to diffuse. The range of validity of the MCT is much limited in comparison with the bulk BLJ. The range of validity in the bulk BLJ is $0.07 < \epsilon < 1.3$ against $0.05 < \epsilon < 0.75$ found in our system. Clearly, the existence of gold nanoparticle has changed the structure of the system and as a result of this structural changes the dynamics of the BLJ particles changes, causing the range of validity of the MCT to decrease. A similar effect has been reported in other systems [29]. We found the MSD curves plotted versus $t\,D(T)$, where the diffusion $D(T)$ is proportional to the inverse of the structural relaxation time $\tau(T)$, to fall onto a master curve for all temperatures in the long α-relaxation regime. The master curve is fitted well by an interpolation formula between the von Schweilder behavior at short rescaled times and the diffusive behavior at long rescaled times. The exponent b is similar for A, B, and C particles within the fit errors. The Stokes-Einstein relation is well obeyed for temperatures well above T_c, where the cooperative processes are insignificant. On supercooling, however, this relation is found to break down, which is due to the presence of critical dynamical fluctuations that are not accounted for in mean-field theories such as the MCT [28,30]. It must be, however, noted that in this paper the effect of a gold nanoparticle composed of 13 gold atoms has been reported on the properties of 1000 BLJ particles (a ratio of 13:1000) in the *NVT* ensemble corresponding to nearly 1% concentration of gold atoms. It would be also interesting to investigate the effect of the nanoparticle size as a control parameter on the properties of the supercooled liquid. Efforts in this direction are underway and will be reported in due course.

ACKNOWLEDGMENT

We thank the Danish Center for Viscous Liquid Dynamics "Glass and Time" for the allotted computer time and resources.

[1] W. Kob and H. C. Andersen, Phys. Rev. Lett. **73**, 1376 (1994).
[2] S. Toxværd, T. B. Schrøder, U. R. Pedersen, and J. C. Dyre, J. Chem. Phys. **130**, 224501 (2009).
[3] U. Bengtzelius, W. Götze, and A. Sjölander, J. Phys. C **17**, 5915 (1984).
[4] W. Götze, J. Phys.: Condens. Matter **11**, A1 (1999).
[5] W. Kob and H. C. Andersen, Phys. Rev. E **51**, 4626 (1995); **52**, 4134 (1995).
[6] M. D. Ediger, C. A. Angell, and S. R. Nagel, J. Phys. Chem. **100**, 13200 (1996).
[7] D. R. Richman and P. C. Charbonneau, J. Stat. Mech. (2005) P05013.
[8] J. P. Bouchaud, L. Cuglaindolo, J. Kurchan, and M. Mezard, Physica A **226**, 243 (1996).
[9] T. R. Kirkpatrick, D. Thirumalai, and P. G. Wolynes, Phys. Rev. A **40**, 1045 (1989).
[10] P. Gallo, R. Pellarin, and M. Rovere, Phys. Rev. E **67**, 041202 (2003); **68**, 061209 (2003).
[11] K. V. Sarathy, K. S. Narayan, J. Kim, and J. O. White, Chem. Phys. Lett. **318**, 543 (2000).
[12] F. W. Starr, T. B. Schrøder, and S. C. Glotzer, Phys. Rev. E **64**, 021802 (2001).
[13] C. Caronna, Y. Chushkin, A. Madsen, and A. Cupane, Phys. Rev. Lett. **100**, 055702 (2008).
[14] C. Roberts, T. Cosgrove, R. G. Schmidt, and G. V. Gordon, Macromolecules **34**, 538 (2001).
[15] M. Kobayashi, Y. Rharbi, L. Brauge, L. Cao, and M. A. Winnik, Macromolecules **35**, 7387 (2002).
[16] W. Götze and L. Sjögren, Rep. Prog. Phys. **55**, 241 (1992).
[17] T. Franosch, M. Fuchs, W. Götze, M. R. Mayr, and A. P. Singh, Phys. Rev. E **55**, 7153 (1997).
[18] S. Sastry, P. G. Debenedetti, and F. H. Stillinger, Nature (London) **393**, 554 (1998).
[19] *Lecture Notes for "Slow relaxations and nonequilibrium dynamics in condensed matter," Les Houches July 1–25, 2002, Les Houches Session LXXVII*, edited by J. L. Barrat, M. Feigelman, J. Kurchan, and J. Dalibard (Springer, Berlin, 2003), pp. 199–270.
[20] S. P. Das, Rev. Mod. Phys. **76**, 786 (2004).
[21] T. A. Weber and F. H. Stillinger, Phys. Rev. B **31**, 1954 (1985).
[22] H. Heinz, R. A. Vaia, B. L. Farmer, and R. R. Naik, J. Phys. Chem. C **112**, 17281 (2008).
[23] www.rumd.org; www.gromacs.org.
[24] S. Erkoc, Physica E **8**, 210 (2000).
[25] Y. Sun, Z. Q. Zhang, K. S. Moon, and C. P. Wong, J. Polym. Sci. B **42**, 3849 (2004).
[26] B. J. Ash, L. S. Schadler, and R. W. Siegel, Mater. Lett. **55**, 83 (2002).
[27] G. J. Papakonstantopoulos, M. Doxastakis, P. F. Nealey, J. L. Barrat, and J. J. de Pablo, Phys. Rev. E **75**, 031803 (2007).
[28] G. Biroli and J. P. Bouchaud, J. Phys.: Condens. Matter **19**, 205101 (2007).
[29] P. Scheilder, W. Kob, and K. Binder, Europhys. Lett. **52**, 277 (2000); **59**, 701 (2002).
[30] S. Davatolhagh and S. Foroozan, Phys. Rev. E **85**, 061707 (2012).